

Impact of the HGF Knockin Microenvironment on Epithelial–Mesenchymal Transition and Cancer Stem Cells in a Non-Small Cell Lung Cancer Xenograft Model

Tony Navas¹, Thomas D. Pfister¹, Scott M. Lawrence¹, Apurva K. Srivastava¹, Robert J. Kinders¹, Suzanne Borgel², Sergio Alcoser², Melinda G. Hollingshead², Lindsay M. Dutko³, Brad A. Gouker³, Donna Butcher³, Elinor Ng-Eaton⁴, Young H. Lee⁵, Donald P. Bottaro⁵, Naoko Takebe⁶, Ralph E. Parchment¹, Joseph E. Tomaszewski⁶, and James H. Doroshow⁶

¹Laboratory of Human Toxicology and Pharmacology, Applied/Developmental Research Directorate, Leidos Biomedical Research, Inc., Frederick National Laboratory for Cancer Research, Frederick, MD 21702; ²Biological Testing Branch, Developmental Therapeutics Program, National Cancer Institute, Frederick, MD 21702; ³Pathology/Histotechnology Laboratory, Laboratory Animal Sciences Program, Leidos Biomedical Research, Inc., Frederick National Laboratory for Cancer Research, Frederick, MD 21702; ⁴Department of Biology, Ludwig Center for Molecular Oncology, Whitehead Institute, Massachusetts Institute of Technology, Cambridge, MA 02142; ⁵Urologic Oncology Branch, Center for Cancer Research, National Cancer Institute, Bethesda, MD 20810; ⁶Division of Cancer Treatment and Diagnosis and Center for Cancer Research, National Cancer Institute, Bethesda, MD 20810



Frederick National Laboratory for Cancer Research

Introduction

Epithelial–mesenchymal transition (EMT) is a cellular process by which epithelial cells acquire mesenchymal, fibroblast-like properties, and display reduced adhesion and increased motility (1). EMT enables tumor cells to invade surrounding tissues and generate distant metastases (Figure 1).

EMT is initiated by the upregulation of transcription factors such as Snail, Slug and Zeb1, which inhibit the expression of E-cadherin in epithelial tumor cells. Recent reports also suggest that the transcription factors Slug and Sox9 cooperate to promote the tumorigenic and metastatic capabilities of human breast cancer cells, thus promoting the characteristics of cancer stem cells (CSCs) in tumors (2).

EMT can be induced by growth factors such as the hepatocyte growth factor (HGF). The HGF/c-Met pathway was recently shown to be activated in small cell lung cancer (SCLC) *in vivo*, and to lead to increased expression of mesenchymal markers as well as tumorigenic and chemoresistant tumor phenotypes (3). The c-Met-specific inhibition of EMT biomarkers reversed the mesenchymal transition and increased chemosensitivity in SCLC.

Recent reports identified CD133, CD44, and ALDH1 as putative surface markers for CSCs in lung tumors. CD133+ cells showed sphere formation, differentiation, and chemoresistance. In non-small cell lung cancer (NSCLC) cells, CD133+ cells express genes involved in stemness, adhesion, motility, and drug efflux (4, 5).

Here, we report that the EMT phenotype is induced in the NSCLC tumor line model NCI-H596 xenograft implanted in a human HGF knockin microenvironment using multiplex quantitative immunofluorescence (qIFA). We detect HGF-induced changes of various EMT transcription and stem cell factors that define changes in the EMT/CSC biology of NSCLC tumor xenografts induced by an HGF stromal microenvironment.

Methods

Reagents Rabbit monoclonal antibodies against 12 EMT transcription factors and cancer stem cell (CSC) markers, including SNAIL, SLUG, SOX9, Gooseoid (GSC), and CD133, were previously generated and characterized (6). Commercial antibodies to CD44v6 (Ms Mab clone 2F10, R&D Systems), NANOG (goat polyclonal, R&D Systems), ALDH1 (RabMab clone EP1933Y; Abcam) and CD133 (Ms Mab AC133 and 293C3, Miltenyi) were used as controls for CSC factor staining. Commercial antibodies to Snail (CST 3879), Slug (CST 9585), and Sox9 (Millipore Ab5535), were used as controls to compare EMT transcription factor staining in FFPE tissues.

Animal models SCID/NCR ("SCID") are immunocompromised mice homozygous for *Prkdc*^{scid} alleles, which are available from Jackson Laboratory for Genomic Medicine (USA). The *Prkdc*^{scid} mutation results in T- and B-cell deficiency, which is the basis for the immunodeficient phenotype. The hHGF^{kn} and hHGF^{kn/ki} mice (*Hgf*^{tm1.100599Prkdc^{scid}/J) harbor either 1 ("hemi-") or 2 ("homozygous") copies, respectively, of the "humanized" knockin mutation (hHGF^{kn}) that replaces exon 3–6 of the endogenous mouse *Hgf* gene with exon 2–18 of the human *Hgf* gene. These mice were implanted with the human cancer cell line NCI-H596 (non-small cell lung carcinoma, ATCC) by subcutaneous injection, and tumors were monitored for tumor growth.}

NCI-H596 The NCI-H596 cell line has been previously reported to contain somatic intronic mutations leading to exon 14 deletion of the MET gene. This mutation leads to decreased Cbl binding in c-Met, prolonged protein stability, extended cell signaling on HGF stimulation, and increased tumorigenicity (7).

Xenograft biopsy and tumor tissue microarrays (TMAs) Whole xenograft tumors were collected by standard dissection methods after they reached 300 mg in weight. Specimens were cut into two to four equal pieces with fine-point scissors or a single-edge scalpel, and immediately flash frozen in a LN₂ pre-cooled, o-ring sealed, conical bottom-screw-capped 1.5-mL Sarstedt cryovial by touching the biopsy to the inside of the tube within one minute of excision. Tubes with frozen tissues or cells were pre-chilled on dry ice and were fixed in 10% neutral buffered formalin for 48 hours (Sigma Aldrich), and were embedded in paraffin before being arrayed using a 1.0-mm core buffered arrayer.

EMT immunofluorescence assay Formalin-fixed paraffin-embedded tissues (FFPEs), including TMAs, were cut into 5 μm sections and placed on slides, and staining was performed in a Bond-max Autostainer (Leica Microsystems). Heat-induced antigen retrieval was performed in Citrate (pH 6.0) at 100°C for 10 minutes. For EMT multiplex IFA detection, directly conjugated rabbit monoclonal antibodies to E-cadherin (clone 36, AF488, BD Biosciences), Vimentin (clone V9, AF790, Santa Cruz Biotechnology), and beta catenin (clone E247D, AF546, Epitomics) were used. Image acquisition was performed using an Aperio FL Scanner and Spectrum Analysis software, as well as a wide-field fluorescent and confocal microscope (Nikon 90i Andor Camera, NIS Elements Software). Image segmentation and quantitative multiplex analysis were performed using Definiens Software (Tissue Studio Architect).

MET immunofluorescence assay Antigen retrieval was performed using Bond Epitope Retrieval Solution 2 (Leica) at 100°C for 10 minutes. Multiplex immunofluorescence was performed on FFPE tumor tissues using 10 μg/mL of rabbit monoclonal anti-pY1235-MET-DIG (digoxigenin, NCI clone 23111) as primary, followed by 10 μg/mL mouse monoclonal anti-DIG-AF546 as the secondary antibody (Jackson Laboratories) and 2.5 μg/mL of rabbit monoclonal anti-total c-MET directly conjugated to AF488 (clone D1C2, AF488, Cell Signalling Technologies).

Additional EMT transcription and CSC factor immunofluorescence analysis EMT multiplex IFA was performed on adjacent tumor tissue sections using the EMT IFA antibody mixture described above but replacing beta catenin with the following unconjugated rabbit monoclonal as the primary antibody: Snail 41-7, Slug 9-12, Sox9 15-4, Gooseoid (GSC) 1-5, or CD133 47-10, and using 10 μg/mL of goat anti-rabbit AF546 (Life Technologies) as the secondary antibody. Additional adjacent sections were stained with commercial antibodies to CD44v6 (AF488), Nanog (AF546), and ALDH1 (AF647) to control for CSC identification in tumor tissues.

Electrochemiluminescent immunoassays of HGF The HGF protein was quantitated using a two-site electrochemiluminescent immunoassay developed for use with a Meso Scale Discovery SectorImager 2400 plate reader, as previously described (8). Antibodies for HGF capture (MAB-694) and detection (AF-294), and a purified recombinant HGF protein reference standard (294-HG) were obtained from R&D Systems. The lower limit of detection for each assay is 0.75 pg/ml in the 96-well format using a 25-μl microtiter sample volume at a total protein concentration of 0.25 mg/ml.

References

- Kalluri and Weinberg. (2009) The basics of epithelial–mesenchymal transition. *J. Clin. Inv.* 119:1420–1428
- Gao et al. (2012) Slug and Sox9 cooperatively determine the mammary stem cell state. *Cell* 148:1015–1028
- Canada et al. (2014) Targeting epithelial-to-mesenchymal transition with Met inhibitors reverts chemoresistance in small cell lung cancer. *Clin. Cancer Res.* 20(4):938–50
- Bertini et al. (2009) Highly tumorigenic lung cancer CD133+ cells display stem-like features and are spared by cisplatin treatment. *Proc. Natl. Acad. Sci.* 106:16261–62
- Alamgir M, et al. (2013) Cancer stem cells in lung cancer: Evidence and controversies. *Respirology* 18:719–734
- Pfister et al. (2013) Development of Recombinant Transcription Factor Proteins and Antibodies for Application in Clinical Immunossays. AACR Annual Meeting, Washington DC, April 6–10, 2013, Abstract# 4544
- Kong-Beltan et al. (2006) Somatic mutations lead to an oncogenic deletion of Met in lung cancer. *Cancer Res.* 66:283–289
- Ahluwalia G, et al. (2006) c-Met ectodomain shedding rate correlates with malignant potential. *Clin. Cancer Res.* 12:4154–62
- Manni et al. (2008) The epithelial–mesenchymal transition generates cells with properties of stem cells. *Cell* 133:704–715

Evaluating EMT in FFPE tissue sections by IFA

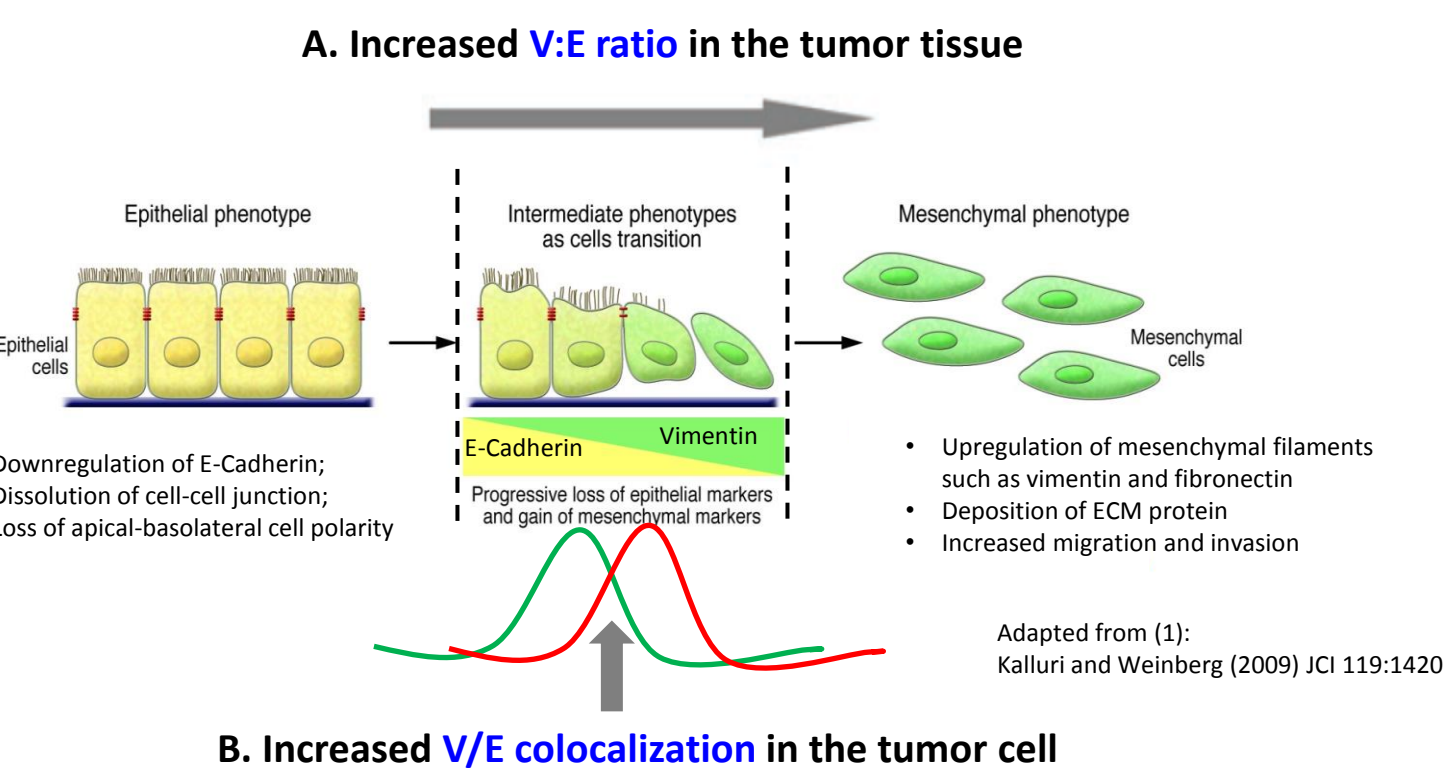


Figure 1. Schematic diagram of epithelial–mesenchymal transition in tumor cells. EMT IFA attempts to capture and measure this complex process by measuring two biomarkers, E-Cadherin and Vimentin, in FFPE tumor tissues. IFA allows us to assess two parameters that correlate with EMT. **A.** Changes in relative expression of both markers in tumor tissues in which Vimentin increases and E-Cadherin decreases with increased transition to the mesenchymal phenotype [V/E ratio]. **B.** Increased colocalized expression of these two distinct markers within the cell defines a narrow transitional zone that captures the apex of the transition: 1) Presence of E-Cadherin (membrane) and Vimentin (cytoplasm) within the same cell, and 2) presence of E-Cadherin and Vimentin on the same pixel area (cytoplasm) [V/E colocalization].

Characterization and selection of EMT and CSC monoclonal antibodies for functional utility studies

Antibody	Clone Name	Predicted molecular size (kD)	Detected over-expressed protein (in cytoplasm)	Detected endogenously expressed protein size (kD)	Detected over-expressed protein (in nucleus)	Model systems used for <i>in vitro</i> studies	Cell Model
anti-GSC	GSC 1-5	*	28	Yes, 36	No	No	HMLE vs. HMLE-GSC
anti-GSC	GSC 32-4	*	28	No	No	No	
anti-GSC	GSC 51-4	*	28	Yes, 20,36	No	No	MCF7-ras vs. MCF7-ras-Sox9
anti-GSC	GSC 58-1	*	28	Yes, 36	No	Yes	
anti-Sox 9	Millipore AB5535	**	56	Yes, 56	Yes, 56	Yes	HMLE vs. HMLE-Slug down-induced
anti-Sox 9	Sox 9 15-4	*	56	Yes, 56	Yes, 56	Yes	
anti-Sox 9	Sox 9 35-11	*	56	Yes, 56	Yes, 56	No	HMLE vs. HMLE-Slug down-induced
anti-Sox 9	CST 9385	**	30	Yes, 36	Yes, 36	Yes	
anti-Slug	CST 9585	*	30	Yes, 30,36	No	No	HMLE vs. HMLE-Slug down-induced
anti-Slug	Slug 2-3	*	30	Yes, 30,36	No	No	
anti-Slug	Slug 9-12	*	30	Yes, 36	No	No	HMLE MCF10a vs. HMLE-Snail down-induced MCF10a-Snail
anti-Snail	CST 3879	**	30	Yes, 36	Yes	Yes	
anti-Snail	Snail 41-7	*	30	Yes, 36	No	Yes	HMLE vs. Nancic
anti-Snail	Snail 41-7	*	30	Yes, 36	No	Yes	
anti-Fox C2	FoxC2 126-9	*	60	Yes, 60	No	Inconclusive	HMLE vs. Nancic
anti-Fox O1	FoxO1 38-2	*	41	No	No	Inconclusive	
anti-Fox O1	FoxO1 46-5	*	41	No	No	Inconclusive	U87 (Low) vs. HT29 (High)
anti-CD133	Miltenyi AC133	**	NP	NP	No (Cyto/PM)	Yes	
anti-CD133	Miltenyi 293C3	**	~97-133	NP	NP	No (Cyto/PM)	HT29 (High) vs. HT29 (Low)
anti-CD133	CD133 47-10	*	~97-133	Yes	Yes	No (Cyto/PM)	
anti-CD133	CD133 133-3	*	~97-133	Yes	Yes	No (Cyto/PM)	

Table 1. Rabbit monoclonal antibody clones were characterized *in vitro* using the selection criteria shown for each column to further select a subset and test for the functional utility in FFPE tissues by IFA. Selected antibodies from each group are highlighted in yellow. * indicates DCTD-NCI/Leidos-produced antibody ** indicates commercial antibody NP = not performed

Immunofluorescence analysis showing endogenous EMT and CSC transcription factor expression on FFPE tissues

Target	Antibody	HMLE (Epithelial)	NAMC8 (Mesenchymal)	Localization
Sox 9	Millipore AB5535	++++	++++	Cytoplasmic/Nuclear
Sox 9	15-4	-	+++	Nuclear
Slug	CST 9585	+++	+++	Nuclear
Slug	9-12	-	+/-	N/A
Snail	CST 3879	-	+	Nuclear
Snail	41-7	-	+	Nuclear
GSC	Abcam 58352	-	-	N/A
GSC	1-5	++++	++++	Cytoplasmic/Nuclear
Target	Antibody	U87 (Negative)	HT29 (Positive)	Localization
CD133	Miltenyi AC133	-	+++	Cytoplasmic/Membrane
CD133	47-10	-	+++	Cytoplasmic/Membrane
CD133	133-3	-	++++	Cytoplasmic/Membrane

Figure 2. Comparative assessment of endogenous EMT/SC transcription factor expression in NAMC8 vs. HMLE tissues or cell pellets using newly generated vs. commercial antibodies by immunofluorescence. HMLE tissues/cells are human mammary epithelial cells (MECs) that had previously been immortalized through the introduction of the HTERT and SV40 early region genes (9). NAMC8 (naturally arising mesenchymal cell) tissues are derived populations of HMLE cells that had spontaneously undergone an EMT and stably resided thereafter in a mesenchymal state. Hence, their phenotypic state was governed by endogenously expressed EMT-TFs. Confocal immunofluorescent image panels show a comparison between endogenous staining of EMT-TFs (brown stain) by DCTD-NCI/Leidos-generated antibodies (left panel) and commercial antibodies (right panel) on NAMC8/FFPE tissues. Table shows a summary of expression levels as well as cellular localization for each EMT-TF using newly generated vs. commercial antibodies in NAMC8 as well as HMLE control tissues. CD133 antibodies were tested for detection of endogenous expression of CD133 by IFA using HT29 vs. U87 cell pellet controls.

hHGF knockin mice express elevated levels of human HGF in plasma and significantly enhanced H596 tumor xenograft growth vs. SCID mice

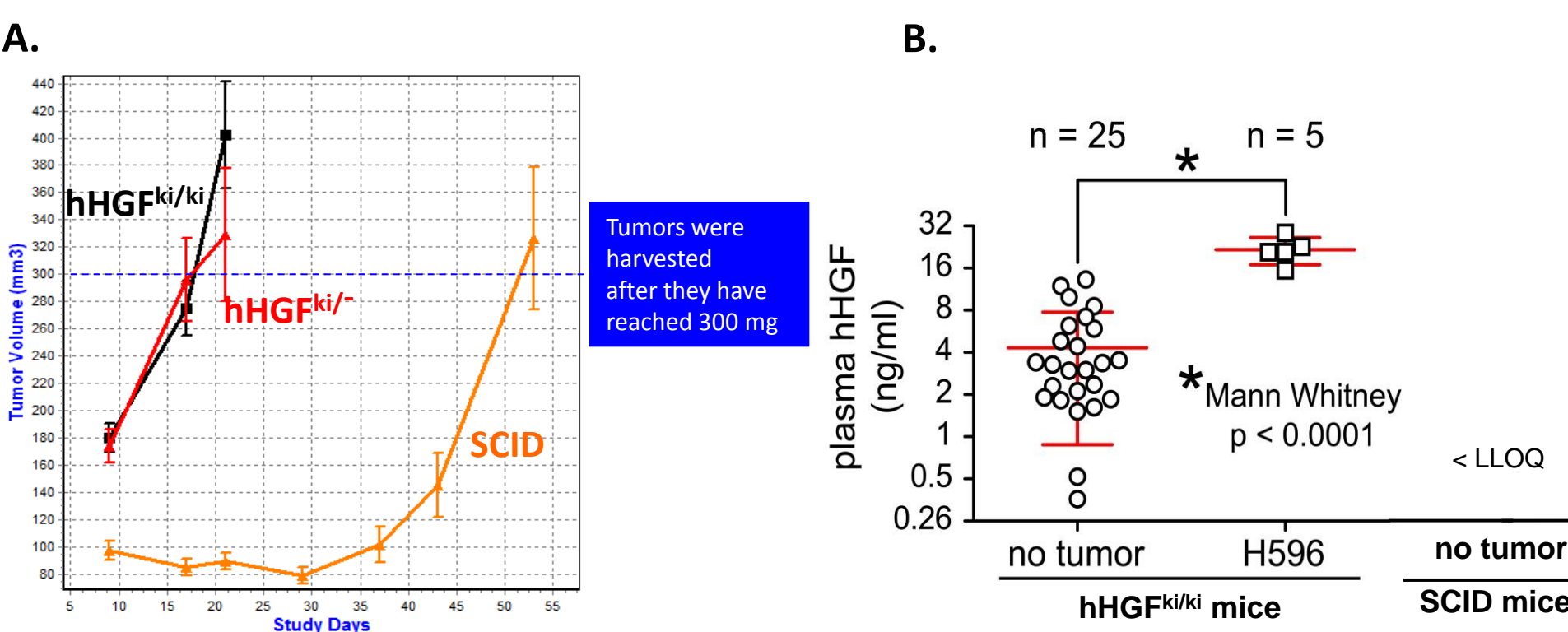


Figure 3. NCI-H596 tumor xenografts exhibit enhanced tumor growth when grown in either a hemi- or homozygous "humanized" HGF transgene (hHGF) that replaces the mouse hepatocyte growth factor (HGF) coding factor in the genome. **A.** H596 cells (1x10⁶) were bilaterally implanted in either SCID, hHGF^{kn}, or hHGF^{kn/ki} mice, and tumor growth was monitored 2–3x/week for the indicated number of days. Tumors were harvested after they have reached 300 mg in tumor weight. **B.** Human HGF (hHGF) is upregulated in the plasma of hHGF^{kn/ki} mice compared to SCID mice. hHGF is enhanced in hHGF^{kn/ki} mice with implanted H596 tumors (1–1.5 cm³ or approx 500–750 mg) compared to control hHGF^{kn} mice with no implanted tumors. The hHGF levels in the plasma of control SCID mouse are below the lower limit of quantitation (LLOQ) for the assay.

Increased epithelial–mesenchymal transition in H596 tumor xenografts from hHGF knockin vs. SCID mice

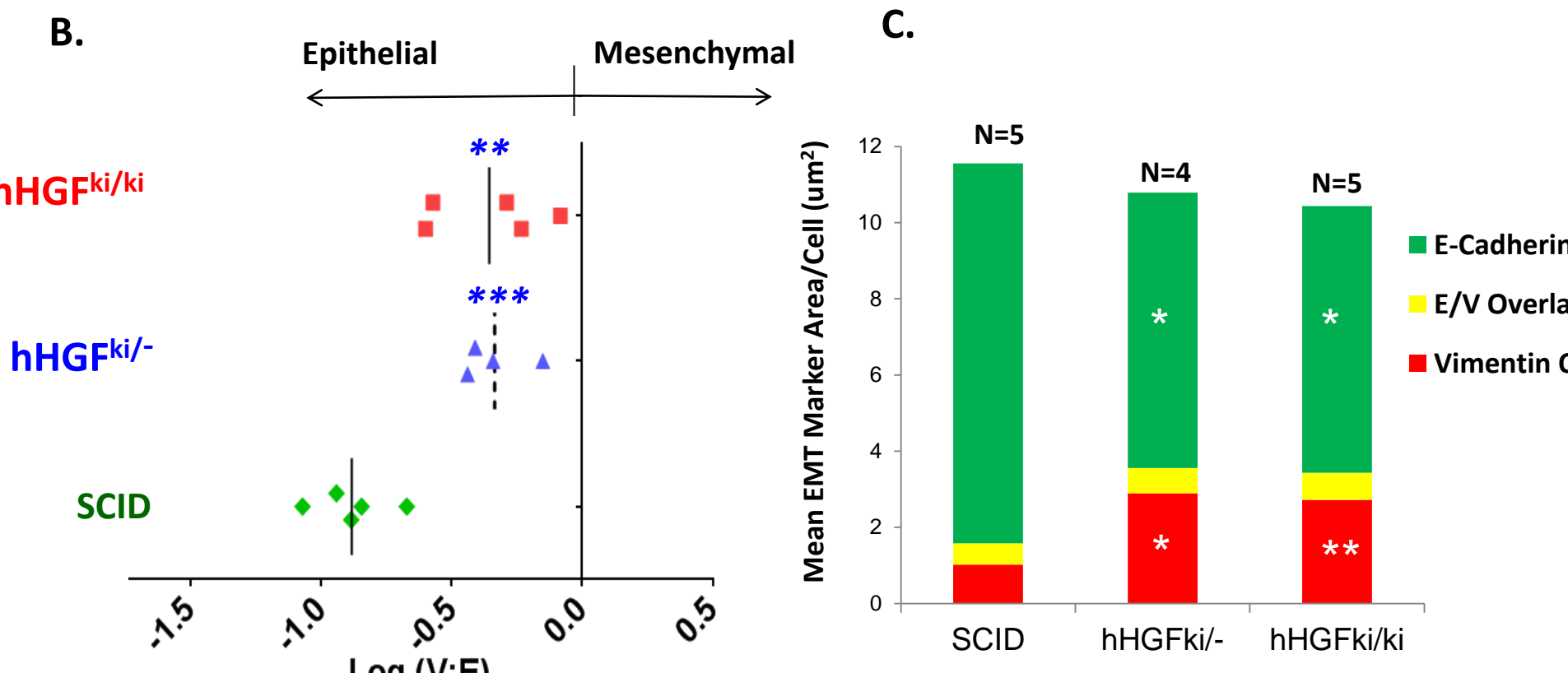
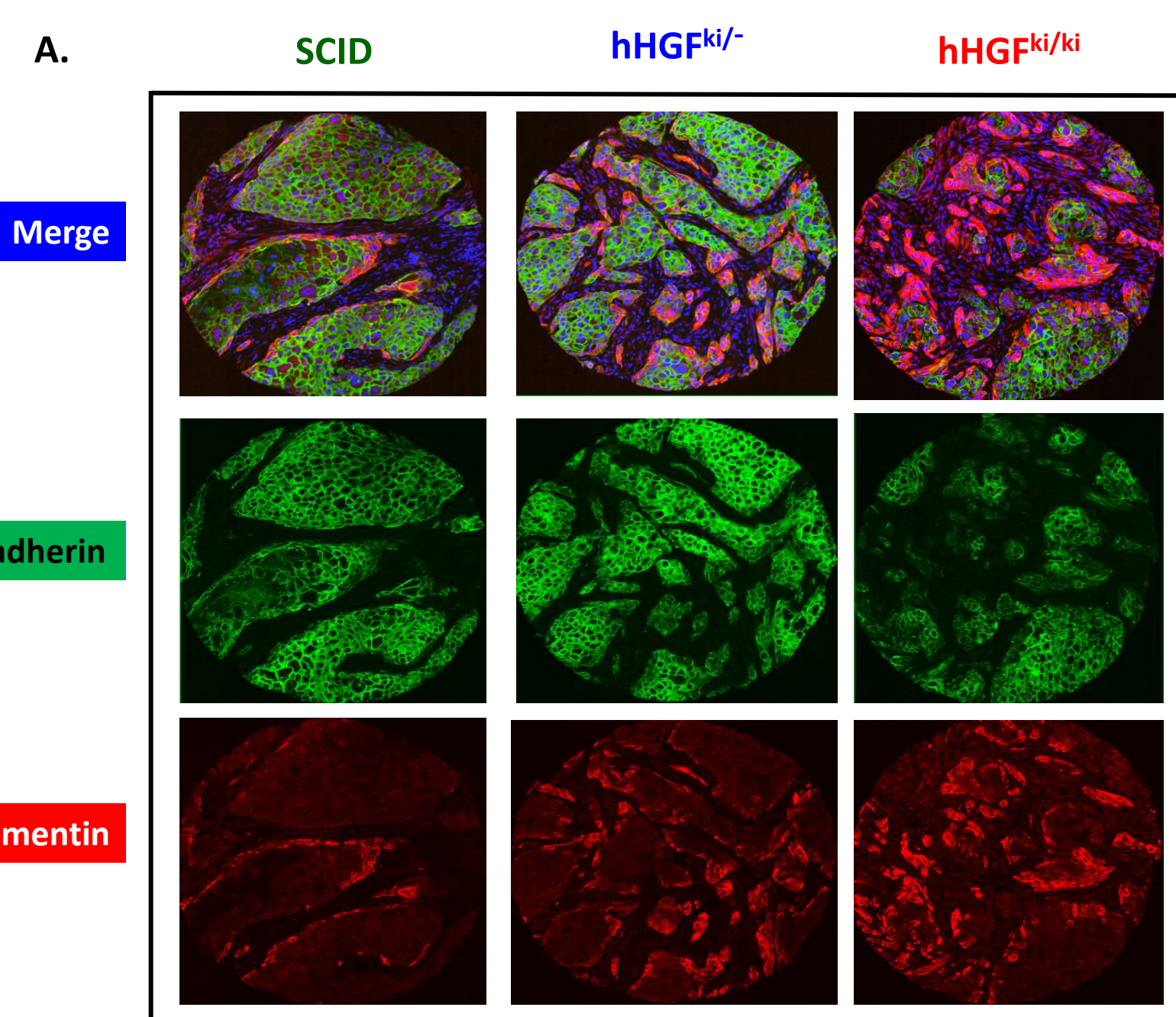


Figure 5. H596 tissues derived from hHGF knockin mice exhibit enhanced epithelial–mesenchymal transition particularly in tumor regions adjacent to hHGF-containing mouse stroma compared to those derived from SCID mice. **A.** Representative immunofluorescence image of TMA tumor tissue derived from hHGF knockin and SCID mice showing the various EMT layers. **B.** Scatter graph shows significant increases in the Vimentin to E-Cadherin ratio in H596 tissues obtained from hHGF knockin mice compared to SCID mice. Each point corresponds to measurements obtained from an individual mouse. *******P*<0.022 vs. SCID; *******P*<0.0006 vs. SCID. **C.** Stacked bar graphs show that the mean expression levels per cell of E-cadherin significantly decreased while that of Vimentin significantly increased in tumors derived from the hHGF knockin compared to SCID mice. **E-cadherin:** *P*<0.050 vs. SCID. **Vimentin:** *P*<0.008 vs. SCID. *******P*<0.050 vs. SCID. A slight increase in E/V colocalization was also observed in tumors from hHGF^{kn} vs. SCID control mice.

This project has been funded in whole or in part with federal funds from the National Cancer Institute, National Institutes of Health, under Contract No. HHSN261200800001E. This research was supported in part by the Developmental Therapeutics Program in the Division of Cancer Treatment and Diagnosis of the National Cancer Institute, and by the American Recovery and Reinvestment Act fund. Frederick National Laboratory for Cancer Research is accredited by the AAALAC International and follows the Public Health Service Policy for the Care and Use of Laboratory Animals. Animal care was provided in accordance with the procedures outlined in the "Guide for Care and Use of Laboratory Animals" (National Research Council, 1996; National Academy Press, Washington, D.C.).

Results

Increased nuclear pY1235-MET expression in H596 xenografts from hHGF knockin vs. SCID mice

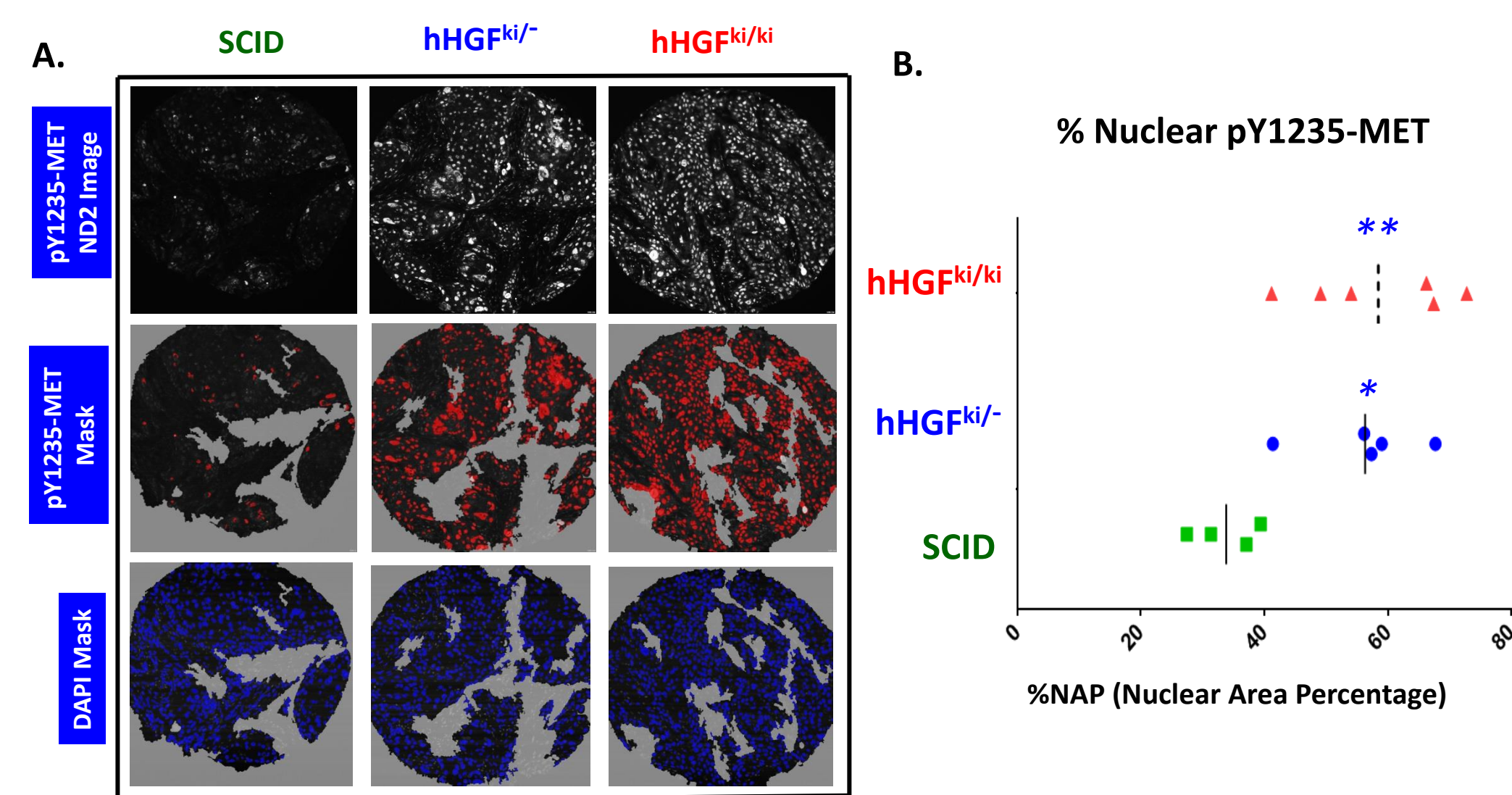


Figure 4. H596 tumor xenografts from hHGF knockin mice exhibit enhanced nuclear pY1235-MET expression compared to tumors obtained from SCID mice. **A.** Top row panel shows representative monochromatic IFA images of TMA tumor tissues derived from hHGF knockin and SCID mice showing pY1235-MET expression. Middle and lower panels show pY1235-MET (red) and nuclei (DAPI, blue) marker masks, respectively, derived from Definiens image analysis. **B.** Scatter graph shows significant increases in pY1235-MET, expressed as %NAP (Nuclear Area Percentage), in H596 tumors obtained from hHGF knockin mice compared to SCID mice. Each point corresponds to measurements obtained from individual mice. *******P*<0.0095 vs. SCID; *******P*<0.016 vs. SCID.

Elevated Slug expression in H596 xenografts from hHGF knockin mice, specifically in tumor regions with reduced E-Cadherin expression and those adjacent to surrounding mouse stroma

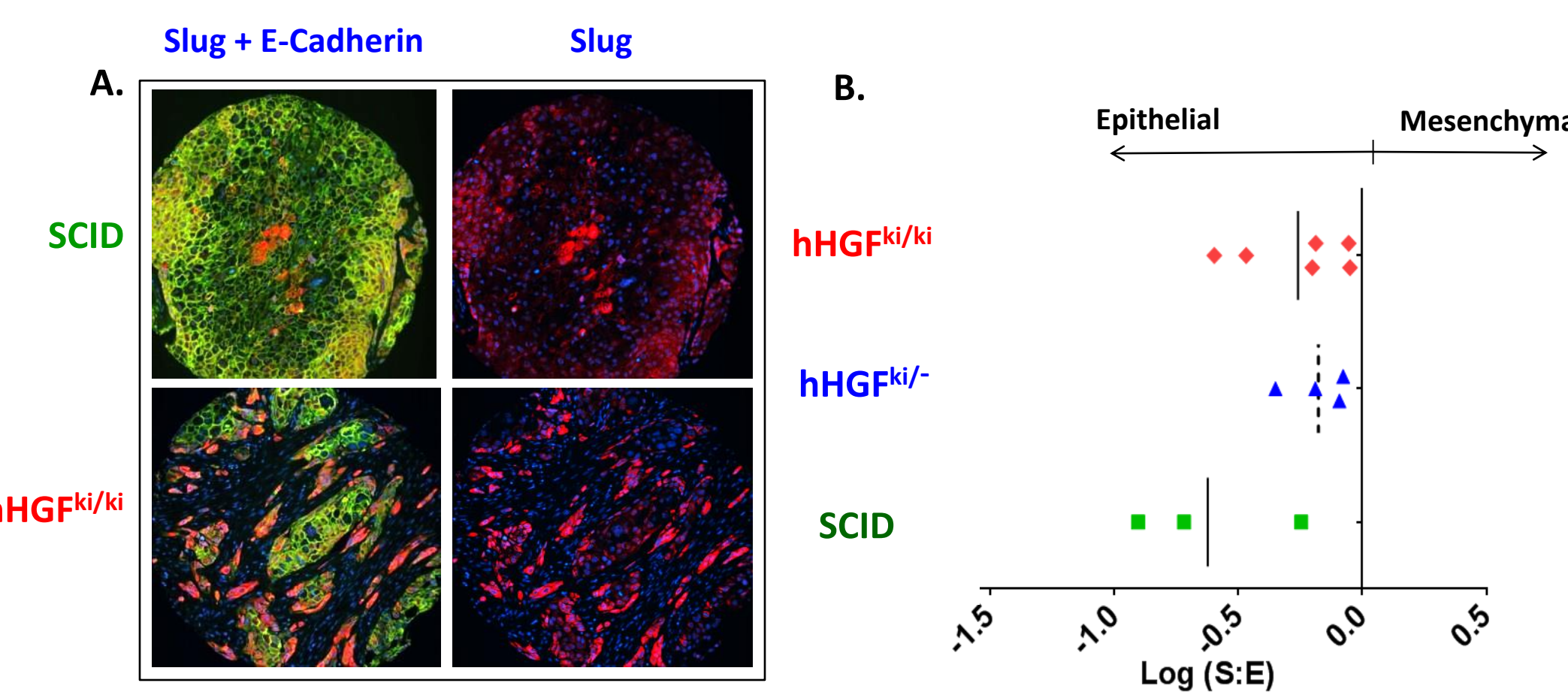


Figure 6. H596 tumor xenografts from hHGF knockin mice exhibit enhanced Slug expression in tumor regions with reduced E-cadherin expression and those adjacent to surrounding mouse stroma. **A.** Representative immunofluorescence image of a TMA tumor tissue derived from hHGF knockin and SCID mice, showing overlapping E-cadherin (green) and Slug (9-12, red) image layers (left panels) or just the Slug image layer (right panels) with DAPI. **B.** Scatter graph shows increases in the Slug to E-cadherin ratio in H596 tumor tissues obtained from hHGF knockin mice compared to SCID mice. This data suggest that upregulated Slug expression is responsible for the downregulation of E-cadherin levels in H596 tumors and this event is most likely driven by factors derived from the hHGF^{kn} mouse stromal microenvironment.

Increased nuclear Snail expression in H596 xenografts from hHGF knockin vs. SCID control mice

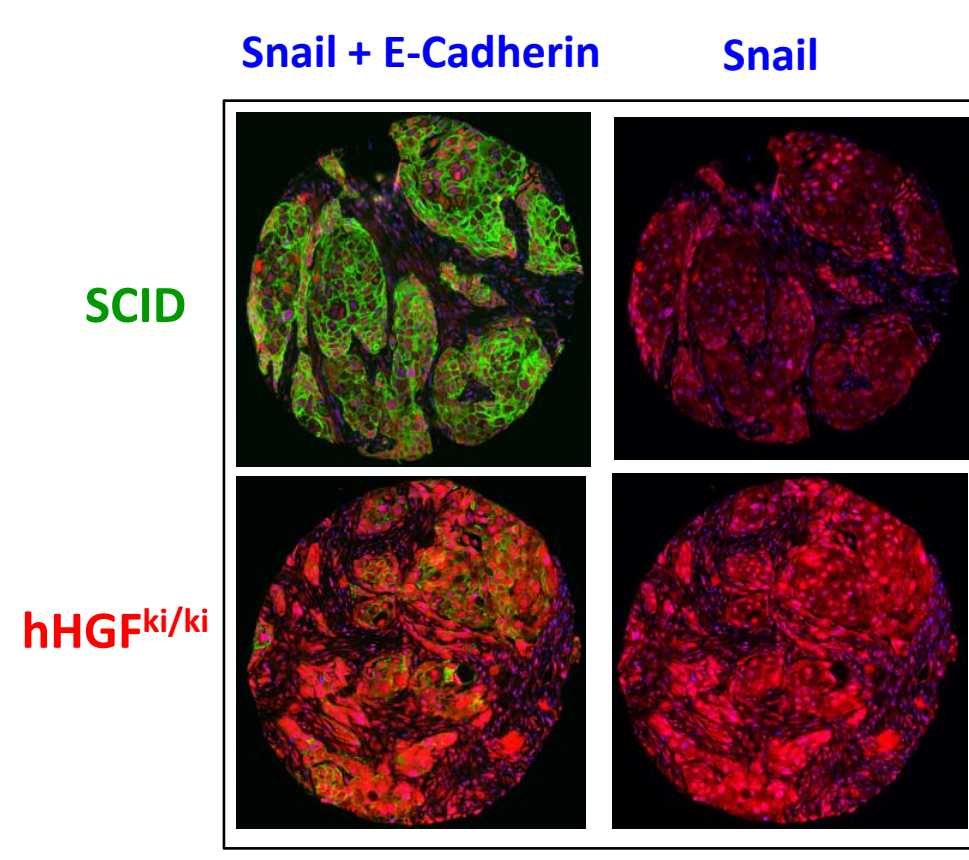


Figure 7. H596 tumor xenografts grown in hHGF knockin mice exhibit enhanced Snail nuclear expression compared to tumors derived from SCID mice. Immunofluorescence image panels show representative TMA tissues derived from hHGF knockin and SCID mice, showing overlapping layers for Snail (41-7) with E-cadherin (in green, left panels) or with just the single EMT-TF layer (in red, right panels) with DAPI. Snail tissue expression shows nuclear localization, and appears to be enhanced in transitioning tumor regions (with diminished E-cadherin staining) adjacent to hHGF-containing stroma, especially in tumors derived from the knockin mice. This data suggest that upregulated expressions of Snail, along with Slug, may be driving EMT in H596 tumors due to the hHGF knockin stromal microenvironment.

CD133 expression is mutually exclusive with Slug in H596 tumors

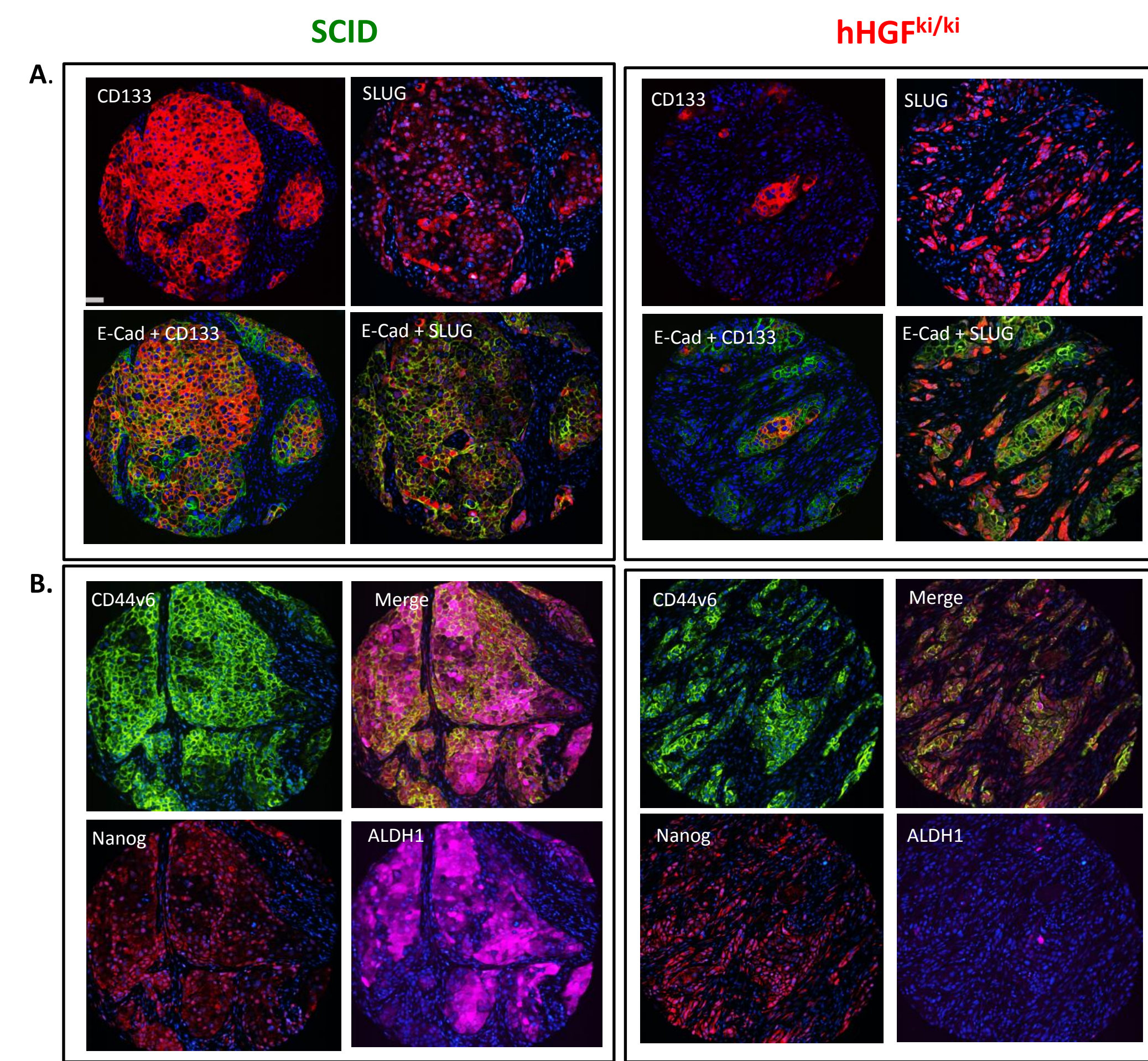


Figure 8. CD133 is expressed inversely as Slug in H596 tumor xenografts. **Figure 8 A and B** show representative multiplex immunofluorescent EMT and/or cancer stemness staining of H596 tumors grown in either SCID or hHGF^{kn/ki} mice. **A.** Two adjacent 5-um tissue sections from each tumor (left and right panels) were stained with E-cadherin and CD133 (47-10) or E-cadherin and Slug (9-12), respectively. IFA images suggest that CD133 is expressed in a majority of cells in H596 tumors grown in SCID mice, but its expression diminishes in tumor cells that have undergone EMT in an hHGF knockin microenvironment, as evidenced by the increased Slug staining in invading cells. Diminished CD133 expression is observed in apparently invasive H596 tumor cells that have upregulated Slug expression. **B.** Other known CSC lung biomarkers such as CD44v6 and ALDH1 are found to be co-expressed in the H596 tumor cells as CD133 in tumors grown in SCID. The expression of these markers appears to be downregulated in tumors derived from hHGF^{kn/ki} mice, suggesting that these markers also become downregulated in cells undergoing EMT in an hHGF knockin microenvironment similar to CD133.

Summary and Conclusions

- Epithelial–mesenchymal transition was induced in H596 tumors when grown in hHGF^{kn/ki} or hHGF^{kn} vs. SCID mice. This is evidenced by the significant increases in Vimentin:E-cadherin ratios as well as increases in the expression of EMT transcription factors Slug and Snail.
- Significant increases in nuclear pY1235-MET (measured by %NAP) were detected in H596 tumors collected from hHGF^{kn/ki} or hHGF^{kn} vs. SCID mice.
- Varying levels of CSC marker expression, including CD44v6, CD133, and ALDH1 were detected in the membrane or cytoplasm of noninvasive regions of H596 tumors in SCID mice and they appear to be diminished in the hHGF knockin microenvironment.
- Slug and Snail expression were increased in transitioning tissue regions that are adjacent to hHGF-containing stroma. The increased expression was coincident with diminished E-cadherin expression and enhanced vimentin expression.
- While Slug expression was predominantly cytoplasmic in invading tumor fronts, the expression was mutually exclusive with CD133 noninvasive regions.
- Snail showed enhanced nuclear expression in tumor cells undergoing EMT.
- This is the first demonstration of EMT and changes in cancer stemness biology in NSCLC induced by an hHGF knockin stromal microenvironment.
- This xenograft model, together with the various pharmacodynamic assays and/or reagents described here, would be useful for testing anti cancer therapeutics that inhibit the c-MET pathway and/or modulate cancer stemness and mitigate tumor metastasis in the clinic.

Acknowledgments

We would like to thank Dr. Robert Weinberg (Whitehead Institute, MIT) for providing invaluable guidance and scientific discussions over the course of this project.